Estimation of photovoltaic production: assessing the performance of large-scale parks

Eduardo Barbosa[a], Agostinho Pinto[b], Bruno Eira[c], Ângela Silva [d], Senhorinha F. C. F. Teixeira[e], Luis Martins[f] and José Carlos F. Teixeira[g]

[a] MEtRICs I&D Centre, School of Engineering, University of Minho,4800-058 Guimarães, Portugal, a95742@alunos.uminho.pt
[b] MEGAJOULE II Consultoria em Energias Renováveis S.A., 4470-105 Maia, Portugal, paulo.pinto@megajoule.pt,
[c] MEGAJOULE II Consultoria em Energias Renováveis S.A., 4470-105 Maia, Portugal, bruno.eira@megajoule.pt
[d] ALGORITMI I&D Centre, School of Engineering, University of Minho, 4800-058 Guimarães, Portugal, asilva@dps.uminho.pt
[e] ALGORITMI I&D Centre, School of Engineering, University of Minho, 4800-058 Guimarães, Portugal, st@dps.uminho.pt
[f] MEtRICs I&D Centre, School of Engineering, University of Minho,4800-058 Guimarães, Portugal, lmartins@dem.uminho.pt
[g] MEtRICs I&D Centre, School of Engineering, University of Minho,4800-058 Guimarães, Portugal, jt@dem.uminho.pt

Abstract:

Accurate energy production estimates are essential for ensuring reliable planning and operation in the photovoltaic sector. This article presents the validation of MEGAJOULE's methodology for estimating PV park energy yield, which combines PVsyst simulations with defined uncertainty ranges for both solar resource and system performance. By comparing simulation-based estimates with real production data from 11 PV parks in Spain over their first four years of operation, the study confirms the robustness of the method. Only six out of 44 evaluated park-years fell outside the predefined uncertainty limits, and the maximum deviation from the average was approximately 5.9%, demonstrating strong agreement between estimated and actual performance.

Keywords:

Photovoltaic systems; Energy yield estimation; PVsyst; Validation.

1. Introduction

The urgent need to reduce greenhouse gas emissions is driving the global energy transition [1]. While fossil fuels remain dominant, significant efforts in renewable energies are increasingly advancing the shift toward a sustainable future. Among these sources, solar energy stands out, particularly PV technology, which directly converts sunlight into electricity, enabling large-scale production and emerging as a viable and competitive alternative to fossil fuels [2].

Photovoltaic energy development is increasingly focused on large-scale solar parks, which play a key role in supplying clean electricity to the grid. These parks consist of arrays of photovoltaic modules that convert sunlight into direct current electricity, which is then managed by system components such as charge controllers, inverters, and transformers to ensure proper conversion, voltage adjustment, and safe distribution to the grid [3]. This process allow solar energy to be efficiently integrated into the electrical system, supporting a continuous and reliable energy supply [4].

A key factor in the planning and operation of photovoltaic plants is the solar resource, whose availability strongly influences system performance [5]. Assessing this resource involves analysing solar geometry, microclimatic, and topographic factors that directly affect energy production. Accurate characterization is crucial during the pre-construction phase for selecting optimal sites and ensuring economic feasibility, as small variations in location can significantly impact energy potential. During operation, continuous monitoring allows for performance tracking, maintenance planning, and more reliable energy production forecasting, ultimately enhancing the efficiency and predictability of photovoltaic systems [6].

Accurate estimation of photovoltaic energy production depends on high-quality solar radiation data. Public and private databases provide historical weather records, satellite-based estimates, or measurements from local

meteorological stations, offering different levels of coverage and precision [7], [8]. While historical and satellite data are suitable for preliminary assessments and long-term analyses, local measurement campaigns deliver precise information adjusted to actual conditions, reducing uncertainty. Climate modelling is increasingly used to generate high-resolution datasets, especially in complex terrains and urban areas where local microclimates, shading, and atmospheric factors strongly influence solar availability [7,9]. Selecting the most appropriate data source is therefore essential to ensure accurate performance predictions and optimize photovoltaic system efficiency.

Estimating photovoltaic energy production involves various models that account for environmental and technical factors. Empirical models, such as the Angstrom-Prescott correlation, use mathematical relationships between solar radiation and meteorological parameters like sunshine duration to provide approximate predictions, but they require calibration for specific locations and have limited precision in complex terrains [12,13]. Measurements from instruments such as pyranometers and pyrheliometers improve accuracy, but in many regions, the limited availability of these data restricts their use. Simulator models, on the other hand, integrate detailed climate data, system characteristics, and operational parameters to provide highly accurate forecasts. Among these, PVsyst is widely used in practice and in this study, offering comprehensive modelling of energy yields, system losses, and overall performance, making it a reliable tool for designing and analysing photovoltaic plants [7,14].

The accuracy of photovoltaic energy production estimates also depends on several environmental and technical factors. Solar radiation, influenced by location, seasons, and climate, is the primary driver of energy output. Module efficiency, inverter performance, ambient temperature, and the angle of solar incidence all affect energy conversion, while shading and soiling can further reduce production. Simulation tools like PVsyst integrate these variables to generate reliable forecasts, highlighting the importance of considering all factors to optimize system performance and ensure accurate energy predictions.

In this study, photovoltaic energy production estimates are based on a Typical Meteorological Year (TMY) dataset provided by Solargis. The TMY condenses several years of meteorological data into a single, statistically representative year, ensuring a realistic characterization of local climatic conditions [10]. It is generated by selecting the most representative months from long-term datasets using cumulative distribution functions, allowing accurate reflection of solar irradiance and temperature patterns [11]. This methodology provides consistent and reliable input data for photovoltaic performance simulations under typical operating conditions.

Within this framework, MEGAJOULE, a consultancy specialized in renewable energy, plays an important role in the early stages of photovoltaic project development. The company focuses primarily on estimating the energy production of solar parks by assessing site conditions, analysing solar potential, evaluating alternatives, and defining system configurations aimed at maximizing energy generation.

This study aims to validate the estimation methodology used in photovoltaic production forecasts by comparing simulated results from PVsyst with actual generation data from operational solar parks. The objective is to assess the accuracy and reliability of the estimates under real operating conditions.

The article is structured into four main chapters. The introduction presents the theoretical framework and introduces the subject to the reader. Chapter 2 describes the case study, the software configuration used to obtain the estimates, and the processing of the results generated through PVsyst. Chapter 3 presents and discusses the results of the annual and seasonal analyses conducted for each park and finally, the conclusions summarize the main findings of the study.

2. Materials and Methods

2.1. Case study

To validate MEGAJOULE's energy production estimation methodology, 11 PV parks located in Aragón, Spain, were analysed. Table 1 summarizes the main technical characteristics of the analysed parks.

The database provided by the company already had some months of missing energy production data, previously removed due to suspected operational issues not documented in the reports. To ensure data quality, additional filtering was applied to remove any remaining non-representative values. Months with availability below 75% were considered outliers and excluded from the analysis to maintain result reliability.

Table 1. *Main characteristics of the PV parks under study.*

Park	Park	Total installed capacity [MWp]	No. of modules	No. of inverters
1	1.10	45.6	133,380	11
2	1.20	49.9	145,800	12
3	1.60	49.9	145,080	12

Park	Park	Total installed capacity [MWp]	No. of modules	No. of inverters
4	1.90	49.9	148,230	12
5	1.60	49.6	143,910	12
6	1.60	49.9	144,540	12
7	1.20	49.9	144,540	12
8	1.40	49.9	144,540	13
9	1.60	49.9	144,540	12
10	1.60	49.9	144,540	13
11	1.60	49.9	144,540	13

Figure 1 presents an overview of the parks' operational and performance characteristics.

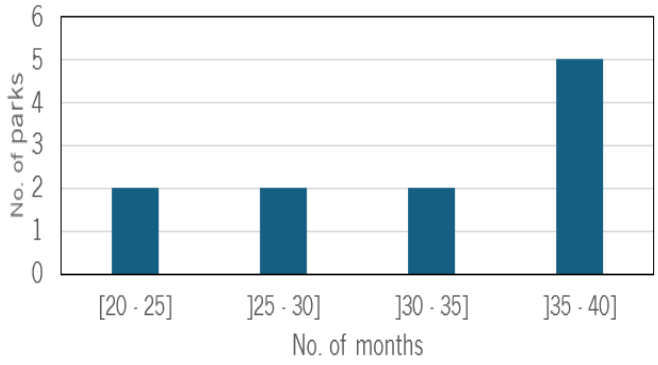

(a)

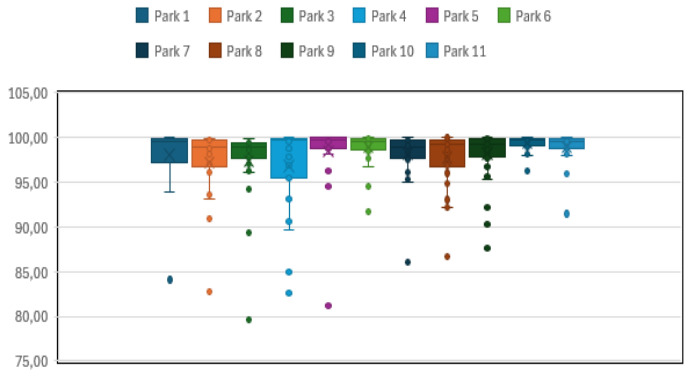

(b)

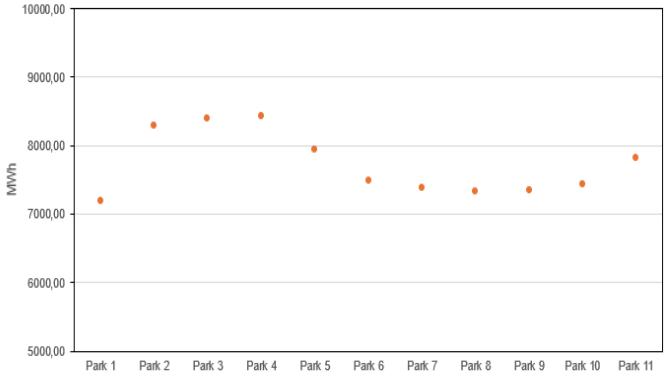

(c)

Figure. 1. *Characterization of the PV parks under study: (a) Months of operation, (b) Availabilities and (c) Real production.*

Figure 1-a) shows the distribution of the photovoltaic parks by operational duration, with most parks having between 35 and 40 months of data. The range is narrow, as the parks started operation around the same time.

Figure 1-b) presents boxplots of park availability, which remains close to 100% for almost all months. This indicates consistently high operational performance across the analysed period.

Figure 1-c) shows the total actual energy production for each park, normalized to 100% availability. The values are very close to each other, reflecting similar conditions across the parks, including location, size, and operational period.

2.2. Software configuration

Performing the simulations in PVsyst was an essential step in the study, as they provided the energy estimates to be validated. The simulations were carried out in accordance with the methodology used by MEGAJOULE, with each project configured to accurately reflect the real characteristics and operating conditions of the respective installation.

In this study, the Solargis TMY dataset was integrated into the PVsyst software as the primary climate database, providing consistent and representative meteorological inputs for energy production simulations.

The parks in this project are all equipped with horizontal N-S single-axis trackers, designed to maximize energy production. These trackers operate within a rotation range of -55º to +55º, allowing the panels to follow the sun's path from east to west throughout the day.

The simulations used backtracking to adjust panel tilt and prevent inter-row shading by slightly reversing the tracking angle when shading was about to occur.

In PVsyst, each park's system configuration comprises the PV modules, inverters, and array layout. The models and quantities of components vary across parks. When multiple module or inverter models are used within a park, sub-arrays are defined, each consisting of a specific module and inverter selected from the database.

2.2.1. Detailed losses

To improve simulation accuracy, it was essential to define the detailed losses affecting energy production, as each parameter influences the final production estimate.

Thermal parameters

The increase in cell temperature can negatively impact the energy production of photovoltaic parks, as thermal behaviour directly affects the system's electrical performance. PVsyst applies a thermal model to estimate heat transfer from the modules based on the temperature difference between the cells and ambient air [15].

In all cases, the option for "free" mounted modules with air circulation is selected, as the photovoltaic modules will be installed on single-axis trackers. This mounting configuration typically allows for better air circulation around the modules, enhancing convective heat dissipation.

Ohmic losses

Wiring losses in the PV array are mainly determined by total circuit resistance, which directly affects power output. PVsyst can estimate these losses in detail based on cable lengths, cross-sections, and distances to the inverter and grid connection points. However, due to limited project data on cable specifications and layout, a default global wiring loss of 1.5% under standard test conditions (STC) was assumed, following MEGAJOULE's methodology summarized in Table 2.

Table 2. *Loss fraction at STC by MEGAJOULE method based on project size.*

Project's Size	Loss Fraction at STC
Up to 10 MW	1.0%
10 – 50 MW	1.5%
> 50 MW	2.0%

Module quality – LID - Mismatch

Module quality loss reflects the confidence in the actual performance of photovoltaic modules relative to the manufacturer's specifications. This is typically determined through factory flash tests, which measure output and define a power tolerance range provided in the datasheets. For each PV park, the specific module datasheet was consulted, and the module quality loss was set at the midpoint of the manufacturer's power tolerance range.

Light-Induced Degradation (LID) is the performance loss that occurs during the first hours of exposure to sunlight in crystalline silicon modules. It results from boron-oxygen (B–O) complexes formed when oxygen dimers in the silicon diffuse, creating parasitic currents that reduce cell output. In the simulations, LID was estimated from the module datasheet's performance warranty graph, with degradation at year 0 representing the LID, as shown in Figure 2 for a GCL module.

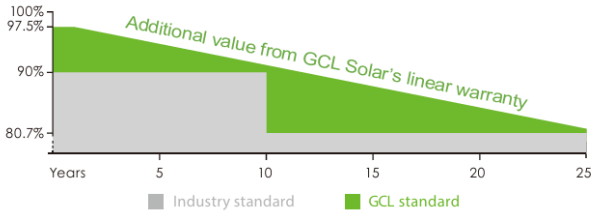

Figure. 2. *Linear performance warranty graph [16].*

Two types of incompatibility losses were considered in the simulations: module mismatch losses and string voltage mismatch losses.

Module mismatch losses occur because modules in an array do not share the same current-voltage characteristics, due to cell thickness variations during manufacturing and uneven solar irradiance causing temperature differences across the array. To consider the losses from this, a mismatch loss of 1.0% was applied in the simulations.

Additional losses occur due to string voltage mismatch, when different strings require different voltages to reach their respective maximum power points. This effect becomes significant only when strings have a different number of modules. Since all strings in the studied cases contain the same number of modules, a 0% loss due to string voltage mismatch was assumed in the simulations.

Soiling losses

Soiling losses occur due to the accumulation of particles on solar modules, which reduces radiation absorption and overall system performance. In the simulations, different loss values were assigned to each park following MEGAJOULE's methodology. The model incorporates a calculation sheet that enables the definition of a customized daily soiling accumulation rate based on local conditions (set at 0.03% per day in this study), to which a fixed monthly value of 0.6% was added to account for soiling from bird droppings. Additionally, two cleaning operations were scheduled, with their dates determined from the analysis of the annual soiling pattern and the hourly precipitation data from the TMY dataset, as illustrated in Figure 3.

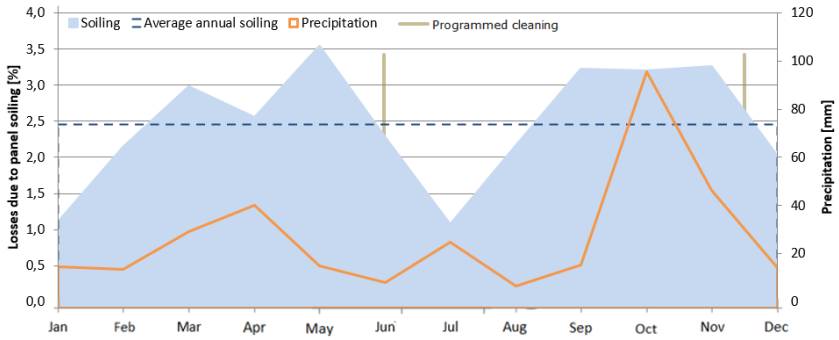

Figure. 3. *Annual soiling pattern for park 1.*

2.2.2. Near and far shadings

In PVsyst, the horizon feature defines large and distant obstacles that may cast shadows on a photovoltaic system, such as mountains, natural landscape features, or tall buildings. For all parks, individual horizon files were generated following the company's methodology, ensuring accurate site characterization prior to importing the data into the software. Figure 4 presents an example of a solar path diagram derived from the horizon definition for Park 1, illustrating the sun's position in the sky throughout the day and across different times of the year. The yellow area represents the range of possible solar positions, while the grey shaded region corresponds to the site-specific horizon profile, highlighting potential obstructions that could limit solar exposure.

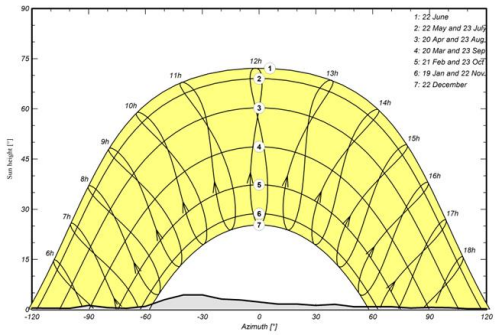

Figure. 4. *Iso-shadings diagram for park 1.*

The project configuration in the software required defining near shading for each park. Although no nearby objects, such as trees, were observed to cause shading during site inspections, near shading still had to be considered to account for shading between the tracker rows themselves.The tracker arrays were modelled according to the actual layout, as shown in Figure 5, with shed areas and module counts adjusted to match the total project capacity while preserving site geometry.

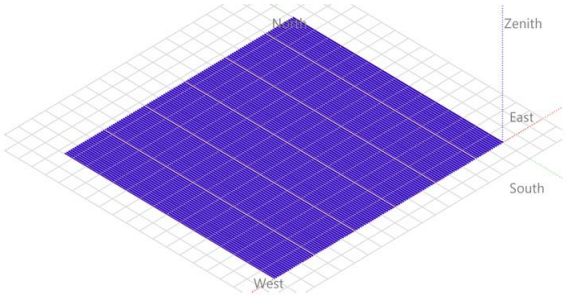

Figure. 5. *Park layout modelled in PVsyst for park 1.*

This configuration ensures that near shading reflects self-shading between tracker rows, and the arrays were divided into partitions representing individual strings to enable accurate simulation of shading and electrical performance.

2.3. Processing PVsyst estimates

The validation of the energy production estimates requires the comparison of itself with the real values of energy produced during the operation of the parks.

For each park, monthly energy production during the first year of operation was estimated using PVsyst. For subsequent years, annual module degradation was applied based on the linear performance warranty graph from the module's datasheet, which was also used to define LID losses. The AD for each module was calculated using the Eq. (1).

$$AD = \frac{P_{initial} - P_{year\ n}}{n} \quad (1)$$

where $P_{initial}$ is the performance after LID in the first year, and $P_{year\ n}$ is the performance in the year n.

PVsyst assumes 100% availability in each simulation. However, actual production values do not reflect this ideal condition, as several factors contribute to reductions in availability, even though the values are often close to 100%. Therefore, it is necessary to apply a correction based on the real availability. For each recorded value of energy production, the gross production will be considered by applying a correction to adjust the real values to reflect an availability of 100%. This results in a corrected actual energy production (E_a), normalized for availability (Av), as expressed in Eq. (2).

$$E_{100\%\ av} = \frac{E_a \times 100}{Av} \quad (2)$$

All the values under analysis were converted into full load hours (FLH) to enable a consistent comparison between different photovoltaic parks, regardless of their installed capacity. This approach provides a normalized measure of energy production by expressing it in terms of equivalent hours at full capacity. In this way, the influence of the total installed power is removed, allowing for a more meaningful assessment of performance across systems of different scales, as shown in Eq. (3). C_{ins} denotes the total installed capacity.

$$FLH = \frac{E_{100\%\ av}}{C_{ins}} \quad (3)$$

Each estimate will be associated with an uncertainty. This uncertainty reflects the potential variability in the estimation process, accounting for factors such as the quality of solar and environmental data, model assumptions, system performance variations, and other technical or operational aspects that may affect the reliability of the results. Equation 4 defines the calculation of the uncertainty limits (L) for each estimate, obtained by adding and subtracting the average production estimate (P50) with the corresponding uncertainty value (Δ).

$$L = P50 \pm \Delta \quad (4)$$

Based on the previously mentioned mathematical model, it was necessary to calculate the uncertainty associated with each estimate for each park. Since the projects are located very close to each other and have similar installed capacities, the uncertainty values obtained are very close, ranging from ±7.46% to ±7.52%. Although the final values differ slightly due to small variations in individual parameter values, they remain within a narrow range.

Although uncertainties were calculated for both one year and the full 20-year period, the one-year values were used for all operational years. This conservative approach accounts for short-term variability at the start of the parks' operation and ensures potential deviations in annual energy production are not underestimated.

3. Results and Discussion

Estimated values were compared with actual data, with annual and seasonal analyses conducted to assess accuracy and identify patterns or discrepancies.

3.1. Annual analysis

The annual analysis presented in Figure 6 compares estimated and actual energy production, corrected for 100% availability and expressed in FLH, for the 11 parks, covering a total of 44 years of operation. In each graph, the blue and orange dots represent the average annual estimated and actual production, respectively, while the vertical lines indicate the range of estimates based on the calculated uncertainty.

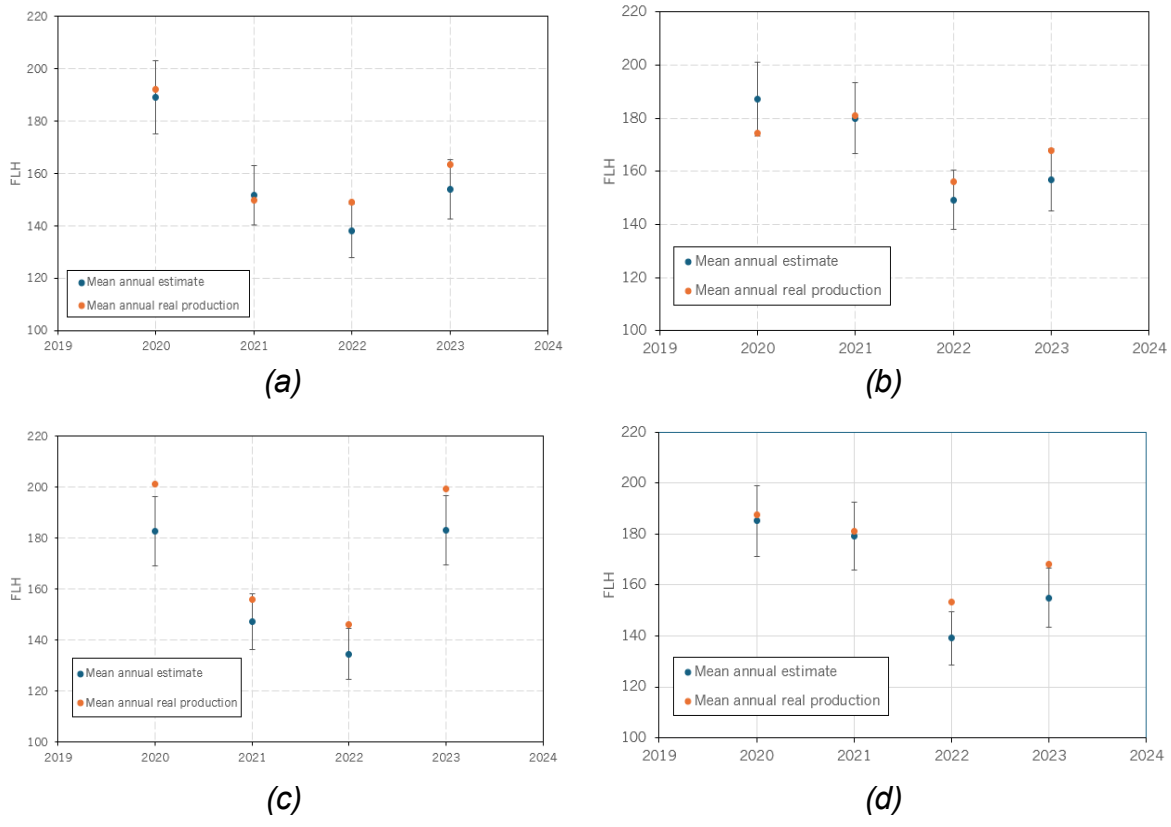

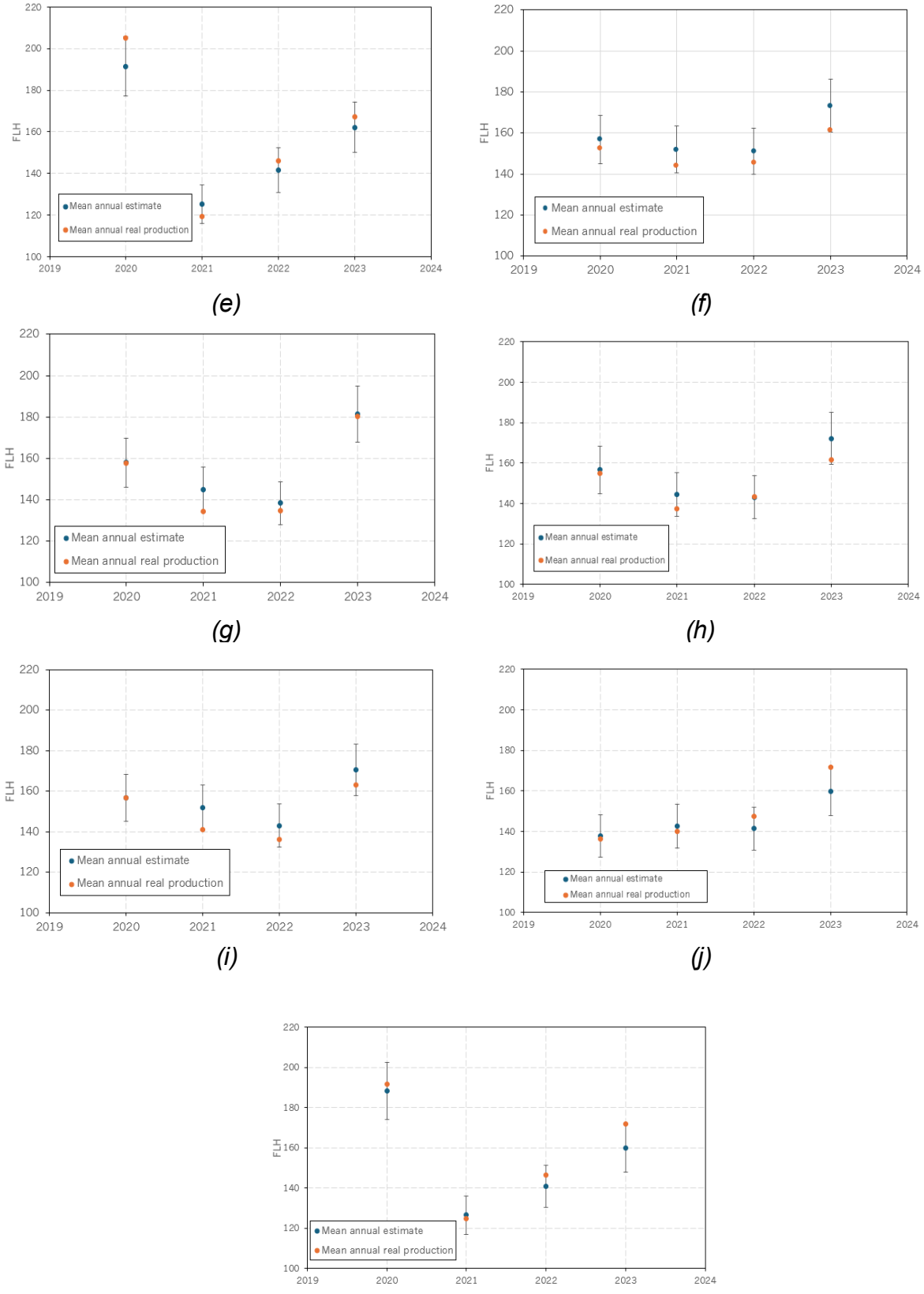

Figure. 6. *Annual analysis of: (a) park 1, (b) park 2, (c) park 3, (d) park 4, (e) park 5, (f) park 6, (g) park 7, (h) park 8, (i) park 9, (j) park 10 and (k) park 11.*

In the annual analysis of the photovoltaic parks, it is expected that the energy estimates gradually decrease over time due to the natural degradation of the modules. However, this trend was not clearly observed in practice. This occurred because the months excluded during the data filtering process are not necessarily the

same each year. As a result, direct comparisons between years are compromised, introducing variability that obscures the expected downward trend in production.

When comparing the estimated values with the actual energy produced, parks 1, 2, 3, 4, 5, 10, and 11 showed higher real production than estimated, with respective differences of 3.42%, 0.91%, 8.50%, 4.78%, 2.81%, 2.45%, and 3.10%.

In contrast, parks 6, 7, 8, and 9 had actual production values lower than the estimates, with respective differences of 4.62%, 2.51%, 3.14%, and 4.06%.

Regarding uncertainty, only parks 1, 3, and 4 had actual production values outside the uncertainty limits, all of which were above the upper bound. Park 1 surpassed the limit in 2022 by 0.52%. Park 3 exceeded the upper limit in three of the four years analysed: 2020, 2022, and 2023, with differences of 2.38%, 1.04%, and 1.32%, respectively. Park 4 exceeded the limit in the last two years of the period, with deviations of 0.09% in 2022 and 0.01% in 2023. This can be observed in Figure 7, where the months with actual values outside the uncertainty range are represented by points lying above the limit lines.

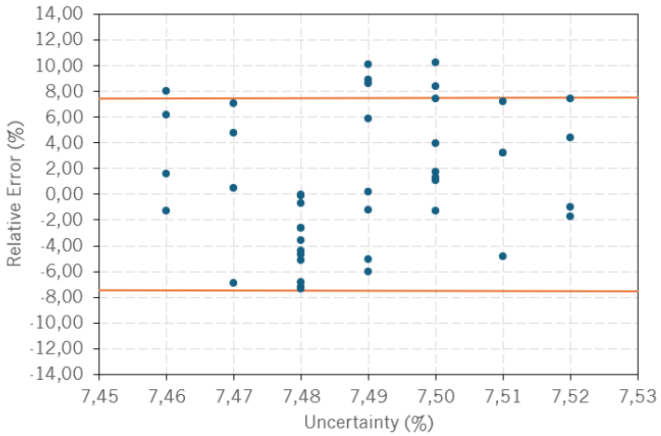

Figure. 7. *Relationship between relative error and estimated uncertainty for the photovoltaic parks under analysis.*

Overall, the estimated values showed good agreement with the actual production results, with most of them remaining within the calculated uncertainty limits. This indicates that the prediction model performed well and was able to closely represent the real behaviour of the parks. Although a few exceptions were identified, where actual production slightly exceeded the upper uncertainty limits in specific parks and years, these cases are isolated and do not compromise the overall quality of the estimates. In conclusion, despite the limitations in comparing different years due to inconsistent data filtering, the yearly analysis demonstrated a positive outcome, with reliable predictions and satisfactory alignment between estimated and measured values.

3.2. Seasonal analysis

In addition to the annual analysis, a seasonal analysis was conducted by grouping data into the four seasons. Figure 8 shows the results for Park 1, which is representative of the entire dataset and exhibits a seasonal behavior similar to the other parks, highlighting the influence of seasonal irradiance patterns on energy production and helping to identify recurring trends.

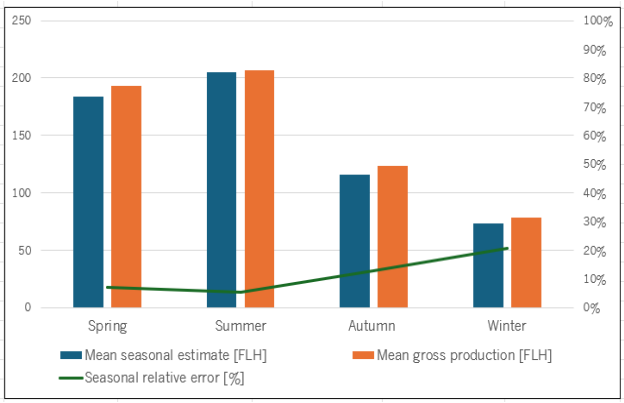

Figure. 8. *Seasonal analysis of park 1.*

As expected, the graphs confirms that energy production is highest during the warmer seasons, with values peaking in spring and summer due to increased solar irradiance. In contrast, production is lower during the colder seasons, autumn and winter. Additionally, Table 3 was created to represent the relative error of the estimates in relation to the actual production values for each season.

Table 3. *Relative errors for each season.*

Season	Spring [%]	Summer [%]	Autumn [%]	Autumn [%]
1	6.9	5.3	12.8	20.7
2	9.8	8.0	3.7	14.4
3	11.3	10.1	7.3	21.9
4	11.4	7.9	5.9	15.1
5	8.8	5.6	5.8	17.7
6	9.4	4.6	7.7	14.1
7	5.6	4.7	7.1	20.8
8	7.7	3.0	7.7	19.4
9	6.0	4.0	8.9	18.7
10	10.7	4.1	6.8	15.3
11	10	5.9	4.2	19.8

The results confirm that energy production is highest during the warmer seasons, with values peaking in spring and summer due to increased solar irradiance. In contrast, production is lower during the colder seasons, autumn and winter.

Winter was the season with the largest differences between estimated and actual energy production. All parks showed significantly higher relative errors in this season compared to the others, reaching 21.9% in the case of Park 3. Even the lowest relative error during winter, observed in Park 6 at 14.1%, was higher than the relative errors recorded in any other season across all parks. This indicates that the estimation methodology appears to be less precise during the winter months.

Regarding the other seasons, it is not possible to identify a single season with consistently lower errors across all parks, as results vary depending on the park under analysis. However, only in Summer and Spring were the lowest values of relative errors recorded compared with the other seasons.

4. Conclusions

The main objective of the present study is to evaluate whether the methodology used by MEGAJOULE to estimate energy production in photovoltaic parks can be validated.

Based on the results obtained from the annual analysis for each park, it can be concluded that the majority of parks perform as predicted. Specifically, 86.4% of the years analysed fell within the calculated uncertainty range, indicating a reliable estimation methodology. In cases where actual production falls outside the uncertainty limits, it consistently exceeds the upper bound, demonstrating that deviations occur only when production is higher than estimated.

Although all deviations beyond the uncertainty range correspond to actual production exceeding estimates, analysis of the relative errors shows a balanced performance of the estimation model. The average RE for years when the estimate is lower than actual production is -4.9%, while for years when the estimate is higher it is 3.6%. Additionally, the number of years with overestimation is similar to the number with underestimation. This symmetry in both error magnitude and frequency confirms that the model is neither systematically oversized nor undersized, demonstrating the reliability and robustness of the estimation methodology.

In summary, the findings of this study validates MEGAJOULE's methodology for estimating energy production, confirming its accuracy when compared to real production data.

Acknowledgments

This work has been supported by FCT within the R&D Units Project Scope: UIDB/00319/2025 (ALGORITMI Center) and R&D Units Project Scope UIDB/04077/2025 (METRICS Center).

Nomenclature

Acronyms

PV	Photovoltaic
TMY	Typical Meteorological Year
N	North
S	South
STC	Standard Test Conditions
LID	Light-Induced Degradation

Latin symbols

AD	Annual degradation, %
Av	Availability, %
C_{ins}	Total installed capacity, MWp
E_a	Actual energy production, MWh
$E_{100\%\,av}$	Production with 100% availability, MWh
FLH	Full load hours
L	Uncertainty limits, FLH
$P_{initial}$	Performance after LID in the 1st year, %
$P_{year\,n}$	Performance in the year n, %
P50	Average production estimate, FLH

Greek symbols

Δ	Uncertainty, %

References

[1] I. Renewable Energy Agency, World Energy Transitions Outlook 2024. 2024. [Online]. Available: www.irena.org

[2] P. Tudor and S.-V. Pușcașu, "MANAGEMENT OF A PHOTOVOLTAIC PARK," 2023. Accessed: Oct. 23, 2025. [Online]. Available: https://www.researchgate.net/publication/376700344_MANAGEMENT_OF_A_PHOTOVOLTAIC_PARK

[3] A. Dixit, A. Saxena, R. Sharma, D. Behera, and S. Mukherjee, "Solar Photovoltaic Principles," in Solar PV Panels - Recent Advances and Future Prospects, IntechOpen, 2023. doi: 10.5772/intechopen.109730.

[4] G. Rajendran, R. Raute, and C. Caruana, "A Comprehensive Review of Solar PV Integration with Smart-Grids: Challenges, Standards, and Grid Codes," May 01, 2025, Multidisciplinary Digital Publishing Institute (MDPI). doi: 10.3390/en18092221.

[5] N. M. Kumar, S. Dasari, and J. B. Reddy, "Availability factor of a PV power plant: Evaluation based on generation and inverter running periods," in Energy Procedia, Elsevier Ltd, 2018, pp. 71–77. doi: 10.1016/j.egypro.2018.07.035.

[6] G. Lobaccaro, M. M. Lisowska, E. Saretta, P. Bonomo, and F. Frontini, "A methodological analysis approach to assess solar energy potential at the neighborhood scale," Energies (Basel), vol. 12, no. 18, 2019, doi: 10.3390/en12183554.

[7] D. Yang, W. Wang, and X. Xia, "A Concise Overview on Solar Resource Assessment and Forecasting," Aug. 01, 2022, Science Press. doi: 10.1007/s00376-021-1372-8.

[8] A. Bansal Bayer, "MEASURING CAMPAIGN EFFECTIVENESS: A PRE AND POST ANALYSIS STUDY OF TEST AND CONTROL GROUPS," 2024. [Online]. Available: https://iaeme.com/Home/issue/IJMHRM?Volume=13&Issue=1

[9] A. I. Bedritskii, R. M. Vil'fand, D. B. Kiktev, and G. S. Rivin, "Roshydromet supercomputer technologies for numerical weather prediction," Russian Meteorology and Hydrology, vol. 42, no. 7, pp. 425–434, Jul. 2017, doi: 10.3103/S1068373917070019.

[10] Solargis, "Time Series and TMY data," 2024. Accessed: Oct. 24, 2025. [Online]. Available: https://kb.solargis.com/docs/time-series-and-tmy-data

[11] T. Cebecauer and M. Suri, "Typical Meteorological Year Data: SolarGIS Approach," in Energy Procedia, Elsevier Ltd, May 2015, pp. 1958–1969. doi: 10.1016/j.egypro.2015.03.195.

[12] K. D. V. Siva Krishna Rao, M. Premalatha, and C. Naveen, "Method and strategy for predicting daily global solar radiation using one and two input variables for Indian stations," Journal of Renewable and Sustainable Energy, vol. 10, no. 1, Jan. 2018, doi: 10.1063/1.4995035.
[13] C. Ekici, "Total Global Solar Radiation Estimation Models and Applications: A review," vol. 2, no. 2, pp. 212–228, 2019, doi: 10.15157/IJITIS.2019.2.2.212-228.
[14] S. Sharma, M. Bukya, and P. Kumar, "PVsyst modeling of 800 kWp capacity grid-tied solar photovoltaic power plant for academic institution," Visions for Sustainability, vol. 2023, no. 20, pp. 175–188, 2023, doi: 10.13135/2384-8677/7941.
[15] PVsyst, "Grid connected systems," 2025. Accessed: Oct. 30, 2025. [Online]. Available: https://www.pvsyst.com/pdf/pdf-tutorials/pvsyst-8/pvsyst-tutorial-v8-grid-connected-en.pdf
[16] GCL, "GCL-P6/72Hxxx," 2016. [Online]. Available: http://en.gclsi.com